Molecular Vision 2017; 23:286-295 <http://www.molvis.org/molvis/v23/286>
Received 15 November 2016 | Accepted 24 April 2017 | Published 26 April 2017

Inhibitory effects of *S100A4* gene silencing on alkali burn-induced corneal neovascularization: an in vivo study

Yu-Lin Wang,[1] Gui-Ping Gao,[1] Yu-Qin Wang,[2] Ying Wu,[1] Zhi-You Peng,[1] Quan Zhou[1]

[1]The Department of Ophthalmology, the First Affiliated Hospital of Nanchang University, Nanchang, China; [2]Zhejiang Eye Hospital, Eye Hospital of Wenzhou Medical University, Wenzhou, China

Objective: The purpose of this study is to explore the inhibitory effects of *S100A4* gene silencing on alkali burn-induced corneal neovascularization (CNV) in rabbit models.

Methods: Sixty-five rabbits were used to establish alkali-induced CNV models. After the operation, rabbits were given daily antibiotic eye drops and an eye ointment to prevent infection. The models were assigned to either an *S100A4* siRNA or an empty vector group. Thirty rabbits were selected as the normal control group. Quantitative real-time polymerase chain reaction (qRT-PCR) was performed to detect the mRNA expression of *S100A4*, vascular endothelial growth factor (VEGF), and tumor necrosis factor-α (TNF-α) in corneal tissues. Immunohistochemistry was used to detect the protein expression of VEGF in corneal tissues, and an enzyme-linked immunosorbent (ELISA) assay was used to detect the protein expression of VEGF and TNF-α in the aqueous humor.

Results: The qRT-PCR results showed that *S100A4* mRNA expression was lower in the *S100A4* siRNA group than in the empty vector group at 1, 3, 7, 14, and 28 days after an alkali burn. When compared with the empty vector group, the expression of VEGF and TNF-α mRNA was downregulated in the *S100A4* siRNA group. The immunohistochemistry results revealed that VEGF protein expression was downregulated in the *S100A4* siRNA group when compared to the empty vector group at 1, 3, 7, 14, and 28 days after an alkali burn. The ELISA results suggest that VEGF and TNF-α protein expression is downregulated in the *S100A4* siRNA group in comparison to the empty vector group at 1, 3, 7, 14, and 28 days after an alkali burn.

Conclusions: These findings indicate that *S100A4* gene silencing can inhibit alkali burn-induced CNV in rabbits.

Ocular injury is the main cause of blindness worldwide, and the majority of ocular injuries result from chemical and thermal burns [1,2]. Eye burns are common and can be caused by various chemical and physical agents, such as acids, alkalis, high temperatures, and fire. These may lead to permanent ocular surface and visual function damage [3]. Eye burns can also cause changes in corneal microstructure. Corneal chemical burns are common ophthalmic injuries that may result in permanent visual impairment [4,5]. Chemical burns represent 7%–10% of eye injuries. Corneal alkali burns are the most dangerous because alkali can penetrate the eye surface very quickly [6]. Corneal alkali burns are considered a common ophthalmologic emergency and account for 7.7%–18% of all ocular traumas. Timely recognition and implementation of the appropriate treatment represent important steps in controlling the progression of early and late complications [3,5]. Current treatments for corneal alkali burns include antibiotics, tear substitutes, sugar cortical hormone, ascorbic acid, collagenase inhibitors, and surgical treatments consisting of penetrating corneal transplantation and amniotic membrane transplantation [6]. In terms of infection, we can observe chemical/thermal burns and pathological corneal neovascularization (CNV) [7]. Despite these advanced therapies, recovery from corneal alkali burns remains a challenge due to the complex mechanisms behind the injury and the variety of cells and molecules involved [8]. A previous study confirmed that *S100A4* expression is increased in the myofibroblasts of regenerating cornea [9].

The *S100A4* gene is located on the rearranged gene cluster of the regular chromosome 1q21 (a is small acidic calcium binding protein (10–12 kDa) exclusively found in vertebrates) [10,11]. As a member of the Ca^{2+} binding protein S100 protein family, *S100A4* is also called mts1, p9Ka, FSP1, CAPL, calvasculin, pEL98, metastasin, 18A2, and 42A. It is composed of at least 21 different members [12-14]. Many human diseases, such as inflammatory diseases, are associated with the altered expression of S100 proteins. *S100A4* also has a strong correlation with inflammation [11,15]. Additionally, S100A4 protein can also be used to stimulate endothelial cell motility [16]. Furthermore, S100A4 is a metastasis-associated protein and is essential in endothelial cells as it inhibits tumor angiogenesis and growth. It also regulates some pro-angiogenic and anti-angiogenic gene

Correspondence to: Yu-Lin Wang, The Department of Ophthalmology, the First Affiliated Hospital of Nanchang University, No. 17, Yongwaizheng Street, Nanchang 330006, Jiangxi Province, China; Phone: +86-791-88692520; FAX: +86-791-88692520; email: exactyulin@163.com

expressions [17]. The *S100A4* gene has a variety of biologic functions, including proliferation and apoptosis, cell motility and adhesion, extracellular matrix remodeling, and the regulation of angiogenesis [12]. A previous study proved that the transfection of *S100A4* can enhance the metastatic potential of bladder and mammary carcinoma cells, thus inhibiting its metastatic potential of cancer [18]. However, there is no relevant research that explores the connection between the *S100A4* gene and CNV in corneal alkali burns. Therefore, our study aims to discuss the inhibitory effects of *S100A4* gene silencing on alkali burn-induced CNV in rabbit models.

METHOD

Construction of S100A4 siRNA expression plasmid: According to the *S100A4* gene sequence in GenBank, the siRNA design principles were used to design the siRNA sequence of the GTGACAAGTTCAAGCTCAA target sequence of the *S100A4* gene. A gene database search confirmed that it had no homology with any other gene sequences. The primer sequences of *S100A4* siRNA were synthesized according to the RNA interference target. They were sense-S100A4:5′-GATCCGTGACAAGTTCAAGCTCAATTCAAGAGATTGAGCTTGAACTTGTCACTTTTTTA-3′ and antisense-S100A4: 5′-AGCTTAAAAAAGTGACAAGTTCAAGCTCAATCTCTTGAATTGAGCTTGAACTTGTCACG-3′. Both synthetic sequences used 10 mmol/L of Tris-HCl (pH8.0) for re-suspension until their concentrations reached 100 μmol/L and their upstream and downstream primers reached a proportion of 1:1. The primers were heated to 95 °C for 3 min and were left at room temperature until they cooled to 37 °C. Subsequently, the primers were linked to a pSilencer 2.1-U6 hygro (donated by Dr. Zhou ZC of the University of Texas MD Anderson Cancer Center, Houston, TX) and digested by BamHI and HindIII double enzymes to construct an S100A4 siRNA expression plasmid. The empty vector pSilencer 2.1-U6 hygro was set as the control. All experimental procedures were conducted in line with the requirements of the relevant animal ethics committee of the First Affiliated Hospital of Nanchang University.

Animal grouping: Ninety-five healthy rabbits weighing 1.8–2.5 kg were purchased from Shanghai Silaike Experimental Animal Co. Ltd. (Shanghai, China). After a slit lamp microscope examination, the rabbit corneas were determined to be normal. Of the 95 rabbits, 30 served as the normal control group and the remaining 65 underwent corneal alkali burns and binocular to serve as the experimental group. The *S100A4* siRNA and empty vector groups each consisted of 30 rabbits that had undergone successful corneal alkali burning and binocular. In the *S100A4* siRNA group, each rabbit was injected with 10 μl of transfection solution made up of an even amount of *S100A4* siRNA expression plasmid and liposome Lipofectamine 2000. This injection was made beneath the 8 quadrants bulbar conjunctiva of the binocular. In the empty vector group, each rabbit was injected with 10 μl of miscible liquids consisting of an even amount of empty pSilencer 2.1-U6 hygro and Lipofectamine 2000. Subsequently, similar injections were made every other day for a total of 4 weeks.

Establishment of alkali-induced CNV model: After the rabbits were dosed with local anesthesia (30 mg/kg of Nembutal) and given 5 g/l tetracaine hydrochloride eye drops, a piece of Whatman III filter paper with a diameter of 10 mm was soaked in a 1 mol/l NaOH solution and placed on the rabbits' eyes for 30 s. Subsequently, corneal and conjunctiva sacs were washed with 100 ml of normal saline, and the CNV model was established with corneal alkali burns. Antibiotic eye drops and ointment were used to prevent infection every day after the operation. Successful criteria for the alkali-induced CNV model was as follows: corneal stroma edema, obvious turbidity, and a subtile iris. Exclusion criteria were: only a slight alkali burn, corneal perforation that occurred after alkali burning, and infection or hyphema that affected CNV observation. A total of 60 rabbits were successfully modeled [19].

Morphological observation of CNV: After one day of modeling, a slit lamp microscope was used to record the time and length of CNV and to calculate the CNV area daily. When measuring CNV, the longest blood vessel with a small continuous bend and CNV growth gravitating toward the center of the corneal opacity was the criterion. Five values were measured in different quadrants of each cornea. Averages were used to record the CNV length of different groups and stages. The A area of CNV was calculated using the Robert computer mathematical model formula ($A=C/12 \times 3.1416 [r^2 - (r-l)^2]$, where C represents the CNV cumulative number of hour circle, r indicates corneal radius (6 mm), and l shows the CNV length from corneal margin to corneal length) [20].

Specimen collection: In terms of specimen collection, six rabbits were randomly selected from the normal control, *S100A4* siRNA, and empty vector groups 1, 3, 7, 14, and 28 days after alkali burning, and 0.1 ml of rabbit aqueous humor was extracted. This was then frozen at −80 °C and an enzyme-linked immunosorbent assay (ELISA) was used to measure vascular endothelial growth factor (VEGF) and tumor necrosis factor-α (TNF-α) protein expression. Subsequently, rabbits were executed using the air embolism method and corneas were cut along the outer edge of the binocular ball under sterile conditions. Corneas from the left eyes were

fixed in 4% poly formaldehyde, dehydrated, and embedded in paraffin, while corneal tissue from the right eyes was frozen at −80 °C for total RNA extraction.

Histopathological detection: Corneas embedded in paraffin were taken out 1, 3, 7, 14, and 28 days after alkali burning and sliced into 5 μm pieces perpendicular to the corneal surface. After normal dewaxing, they were dyed with common hematoxylin and eosin (HE), and the pathologic morphology of the corneas was observed under an optical microscope.

Immunohistochemical staining: Corneas embedded in paraffin were taken out 1, 3, 7, 14, and 28 days after alkali burning and sliced into 5 μm pieces perpendicular to the corneal surface. After normal dewaxing and flushing with phosphate buffered saline (PBS), they were immersed in 0.01 ml ethylenediaminetetraacetic acid (EDTA; pH 8.0) to repair antigens. The normal goat serum was sealed for 3 min at room temperature. Mouse anti rabbit VEGF antibody (1:100, American Abcam Corporation,Cambridge, MA) was incubated overnight at 4 °C. After PBS flushing, the second antibody of biotin goat anti mouse (Wuhan Boster Biologic Technology., Ltd., Wuhan, Hubei, China) was incubated for 20 min at room temperature. After flushing three times with PBS, a horseradish peroxidase labeled streptavidin solution was incubated for 10 min at room temperature. The diaminobenzidine (DAB) was visible for 5 min after PBS flushing. Subsequently, the sections were completely washed and nucleus was re-dyed with hematoxylin for 30 s (with full washing). Next, the sections were differentiated with 1% hydrochloric acid alcohol dehydrated with alcohol, transparented with xylene and sealed with resinene. VEGF expression was observed under a microscope and pictures were taken. Criteria for the immunohistochemical staining were that the cytoplasm, cell membrane, or nucleus was brownish yellow. This indicates a positive result. VEGF staining was used to integrate the integral optical density (IOD) analysis conducted using Image Pro Plus 6.0 software. Each slice was randomly selected from six fields of view for quantitative analysis.

Quantitative real-time polymerase chain reaction (qRT-PCR): Corneal tissues of each group were taken out of the freezer 1, 3, 7, 14, and 28 days after alkali burning and total RNA was extracted using Trizol reagent (Invitrogen Inc., Carlsbad, CA, USA). A reverse transcription kit (Tiangen Biotechnology Co. Ltd, Beijing, China) was used to transcript total RNA into cDNA. The following specific experimental procedures were followed. SYBR Green I fluorescent dye (Applied Biosystems, Inc., Foster City, CA) was applied to conduct the qRT-PCR. The reaction system of each gene was 20 μl: 10 μl 2 × SYBR Green, 0.3 μl of upstream and downstream primers (20 μM), 1.0 μl cDNA, and 8.4 μl ddH_2O. The reaction conditions were: 95 °C for 5 min, 95 °C for 30 s, and 60 °C for 1 min (40 cycles in total). β-actin served as an internal reference. The primer sequences are shown in Table 1. The relative expression of *S100A4*, VEGF, and TNF-α in each group and at the different time points was performed using the following formula: $n = (1+E)^{-\Delta\Delta CT}$ [21]. E indicates the amplification efficiency of the target gene primer ($E=10^{-1/\text{Standard curve slope}}$) [22]. In this experiment, the primer amplification efficacy was calculated as $\Delta CT = (CT_{\text{target gene}}-CT_{\beta\text{-actin}})$.

ELISA assay: The aqueous humor was taken out from the −80 °C frozen corneas 1, 3, 7, 14, and 28 days after alkaline burning. The protein expression of VEGF and TNF-α in the aqueous humor was detected using a rabbit VEGF ELISA kit (Srkbio (sh) Ltd., Shanghai, China) and a TNF-α ELISA kit (Elabscience Biotechnology Co., Ltd, Wuhan, China). Procedures were conducted according to the kits' instructions. The optical density (OD) value of each hole was measured at the wavelength of 492 nm and a standard curve was drawn using the OD values of standard products at different concentrations. The concentrations of VEGF and TNF-α protein were found to have a standard curve (according to OD values).

Table 1. RT-qPCR primer sequences of S100A4, VEGF, TNF-α and β-actin.

Gene		PCR primer sequence
S100A4	Sense	5′-GGGCAAAGAGGGTGACAAGTTC-3′
	Antisense	5′-CTGGGCTGCTTATCTGGGAAG-3′
VEGF	Sense	5′ -CTTGCTGCTCTACCTCCACC-3 '
	Antisense	5 ' -CTTTGGTCTGCATTCACATTTG-3′
TNF-α	Sense	5 '- ATGAGCACGGAAAGCATGATCC - 3′
	Antisense	5′- AGGGCAAGGCTCTTGATGGCAG - 3′
β-actin	Sense	5′ -CTACAATGAGCTGCGTGTGG-3′
	Antisense	5′ -TAGCTCTTCTCCAGGGAGGA-3′

Notes: RT-qPCR, quantitative real-time polymerase chain reaction; VEGF, vascular endothelial growth factor; TNF-α, tumor necrosis factor-α.

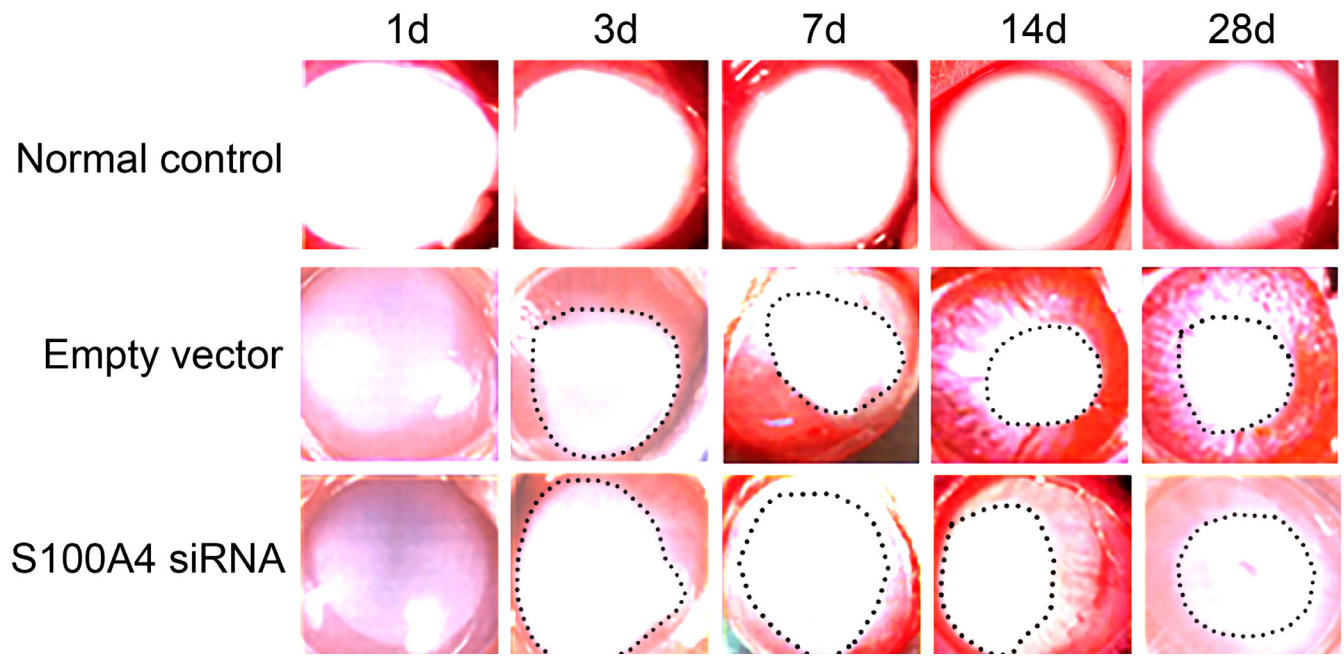

Figure 1. Growth of CNV after alkali burns at each time point (× 400). Notes: The dotted line represents the edge of CNV; CNV, corneal neovascularization.

Statistical analysis: SPSS 13.0 statistical software (SPSS Inc., Chicago, IL) was used for data analysis and measurement. Data are expressed as mean ± standard deviation (± SD). The differences between each time point in each group were analyzed using one-way analysis of variance (ANOVA). The pairwise comparison was tested using the Newman–Keuls test. The difference was considered to be significant when $p<0.05$.

RESULTS

Growth condition of CNV in each group: As shown in Figure 1, CNV did not occur in the corneal tissues of the empty vector and the *S100A4* siRNA groups 1 day after alkali burning. Varying degrees of edema were seen in the corneal epithelial 3 days after burning. This was followed by corneal opacity and limbal vascular network filling. Additionally, the growth of CNV in the limbus was seen to have a lower density of blood vessels compared to the central cornea. In the first 3–7 days after alkali burning, vigorous CNV growth was detected in the empty vector group. Seven days after alkali burning, CNV density was increased significantly. Fourteen days after alkali burning, CNV in the empty vector group significantly increased, forming significant anastomosis and a loop-like vascular network that almost covered the entire cornea. After the area of CNV decreased, the partial vascular started shrinking and disappearing. Twenty-eight days after alkali burning, the mature blood vessels in the corneal tissues of the empty vector group displayed a lower vascular density compared to day 14 after burning. CNV growth was relatively slower in the *S100A4* siRNA group 7, 14, and 28 days after alkali burning than in the empty vector group. The length and area of CNV was also significantly less than those recorded in the empty vector group. No CNV developed at any time point in the normal control group.

The length and area of CNV was significantly smaller in the *S100A4* siRNA group than in the empty vector group at each time point (all $p<0.05$). Fourteen days after alkali burning, the area was significantly larger than the area at any other time point in the normal control and empty vector groups (Table 2).

Histopathological changes of corneal tissues in each group: A few inflammatory cell infiltrations were observed upon HE staining in the empty vector group 1 day after alkali burning. However, there were many mononuclear inflammatory cell infiltrations, matrix structure disorder, and the formation of CNV in the superficial corneal stroma and epithelial cell layer 3 days after alkali burning. Seven days after alkali burning, a larger CNV cavity developed in the corneal stroma. This was also accompanied by infiltration of the macrophages, neutrophils, monocytes, and other cells. Additionally, 14 days after alkali burning there was an increased inflammatory response, CNV volume, thickened lumen, and a red blood

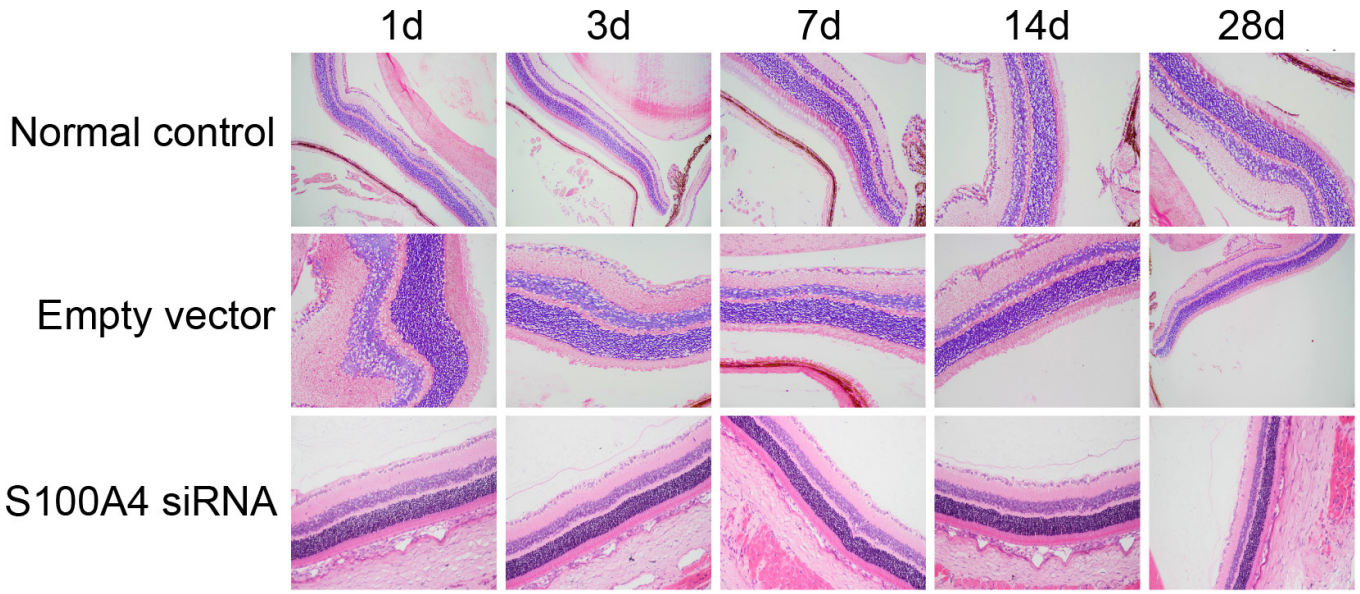

Figure 2. HE staining in corneal sections after alkali burn (× 40). Note: HE, haematoxylin eosin.

cell infiltration in part of the CNV cavity (within the corneal stroma). Twenty-eight days after alkali burning, inflammation and CNV density decreased, revealing thick, visible, mature vessels. Inflammatory cell infiltration and CNV density were lower in the *S100A4* siRNA group than in the empty vector group. No inflammatory reaction was observed in the normal control group at any time point (Figure 2).

The mRNA expression of S100A4, VEGF, and TNF-α in the corneal tissues of each group: The qRT-PCR results indicate that in the empty vector group the mRNA expression of *S100A4* first increased and then gradually returned to normal levels along with CNV growth (Figure 3A). The mRNA expression of *S100A4* peaked 7 days after alkali burning and then gradually decreased from day 14 onwards, reaching a normal level at day 28. This result indicates that *S100A4* gene expression is consistent with the growth and regression of CNV. The mRNA expression of *S100A4* was lower in the *S100A4* siRNA group than in the empty vector group (Figure 3A, $p<0.01$). No significant difference was observed between the normal control and empty vector groups. The mRNA expression of VEGF and TNF-α also increased at first and then gradually returned to normal levels in the empty vector group. This trend was also consistent in the *S100A4* siRNA group; however, the mRNA expression of VEGF and TNF-α w was lower in the *S100A4* siRNA group at each time point when compared to the empty vector group (Figure 3B–C, $p<0.05$). This suggests that *S100A4* affects CNV by regulating the expression of VEGF and TNF-α.

Expression of VEGF protein in the corneal tissues of each group: The immunohistochemical staining results show that the expression of VEGF protein at each time point was lowest in the normal control group. There was an increased

Table 2. The comparison of the corneal neovascularization length and area after alkali burn.

Index	Group	Time points after alkali burns			
		At 3 days	At 7 days	At 14 days	At 28 days
Length (mm)	Norma control group	0±0	0±0	0±0	0±0
	Empty vector group	0.92±0.08**	1.99±0.49**	4.22±0.60**	3.07±0.38**
	S100A4 siRNA group	0.82±0.06**#	1.33±0.32**#	3.11±0.42**##	2.18±0.25**##
Area (mm^2)	Norma control group	0±0	0±0	0±0	0±0
	Empty vector group	12.68±3.24**	32.44±6.59**	72.23±9.66**	49.23±4.18**
	S100A4 siRNA group	8.26±2.65**#	25.11±3.56**#	55.52±7.54**##	39.29±4.24**##

Note: ** refers to $p<0.01$ when compared with the normal control group; # and ## refer to $p<0.05$ and $p<0.01$ when compared with the empty vector group.

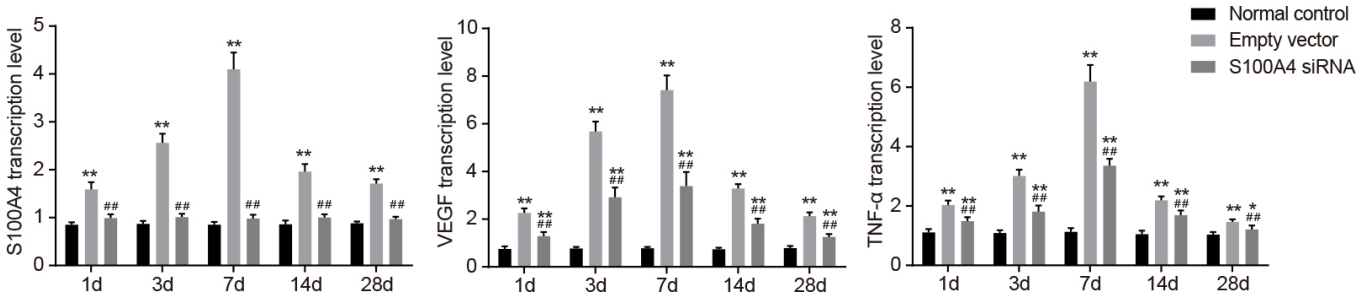

Figure 3. The mRNA expressions of S100A4, VEGF, and TNF-α after alkali burns at each time point for each group. Notes: mRNA, microRNA; VEGF, vascular endothelial growth factor; TNF, tumor necrosis factor; * and ** refer to p<0.05 and p<0.01, respectively when compared with the normal control group; # and ## refer to p<0.05 and p<0.01, respectively when compared with the empty vector group.

expression of VEGF protein in the corneal epithelium 1 day after alkali burning in the empty vector group. However, no VEGF protein expression was found in the corneal stroma. VEGF protein expression in the *S100A4* siRNA group was significantly lower than that in the empty vector group [VEGF IOD in the cornea (72.5±5.5)/(82.1±7.3), p<0.05]. In the empty vector group, the corneal epithelial thickened and VEGF expression increased in the corneal epithelium and stroma 3 days after alkali burning. However, no VEGF expression was found in the *S100A4* siRNA group. In addition, the VEGF IOD in the corneas of the *S100A4* siRNA group was significantly lower than that in the corneas of the empty vector group [(88.3±9.1)/(102.4±5.2), p<0.01]. Seven days after alkali burning, VEGF protein expression was high in the corneal layer of the empty vector group, and brown particles were detected in the corneal epithelium, the vascular endothelial cells, and the inflammatory cells of the corneal stroma. In the *S100A4* siRNA group, VEGF protein expression in the corneal epithelium, vascular endothelial cells, and inflammatory cells of the corneal stroma was significantly lower than in the empty vector group [VEGF IOD in the cornea (129.5±11.0)/(151.7±13.7), p<0.01]. In the empty vector group 14 days after alkali burning, the corneal epithelial thickened to a greater degree than the 7-day measurement, and there was a decrease in VEGF protein expression and VEGF IOD (112.4±6.2). VEGF protein expression in the corneal epithelial of the *S100A4* siRNA group decreased more than in the empty vector group, with VEGF IOD at 97.2±8.7 (p<0.01). Twenty-eight days after alkali burning, the expression of VEGF protein in the corneal epithelial and stroma was still visible in the empty vector group. However, VEGF protein expression was low in the intravascular red blood and vascular endothelial cells. VEGF protein expression in the *S100A4* siRNA group at various time points was significantly lower than that in the empty vector group [VEGF IOD: (79.7±5.3)/(87.1±4.2), p<0.05]. There was no positive expression of VEGF in the corneal stroma or vascular endothelial cells of the *S100A4* siRNA group (Figure 4, Table 3).

The protein expression of VEGF and TNF-α in the aqueous humor of each group: An ELISA assay was used to detect the VEGF and TNF-α protein levels in the rabbits' aqueous humor. The results showed that VEGF protein concentration did not change in the normal control group over time. However, the VEGF protein concentration in the aqueous humor of the empty control and *S100A4* siRNA groups was significantly higher than that in the aqueous humor of the normal control group (p<0.05 or p<0.01). The VEGF protein concentration increased gradually, peaked at day 7, and gradually decreased thereafter. In the *S100A4* siRNA group, VEGF protein concentration in the aqueous humor was significantly lower than that in the aqueous humor of the empty control group at every time point (p<0.05 or p<0.01; Figure 5). TNF-α protein and VEGF protein had similar expression trends in each group. TNF-α protein concentration in the empty control and *S100A4* siRNA groups were significantly higher than in the normal control group (p<0.05 or p<0.01). Furthermore, TNF-α protein concentration in the *S100A4* siRNA group was significantly lower than that observed in the empty control group (p<0.05 or p<0.01; Figure 6).

DISCUSSION

Corneal alkali burns are considered common ophthalmologic emergencies that can result in devastating complications [3]. Pathological CNV is associated with inflammation due to infection or chemical burns [8]. Despite the fact that blood vessel growth can repair some of its effects, CNV and hyperpermeability may lead to impaired vision and transplantation failure [23].

In this study, we found that the level of *S100A4* in the siRNA group was significantly lower than that in the empty vector group. This indicates that *S100A4* is essential in the repair of corneal alkali burns. We also found that *S100A4*

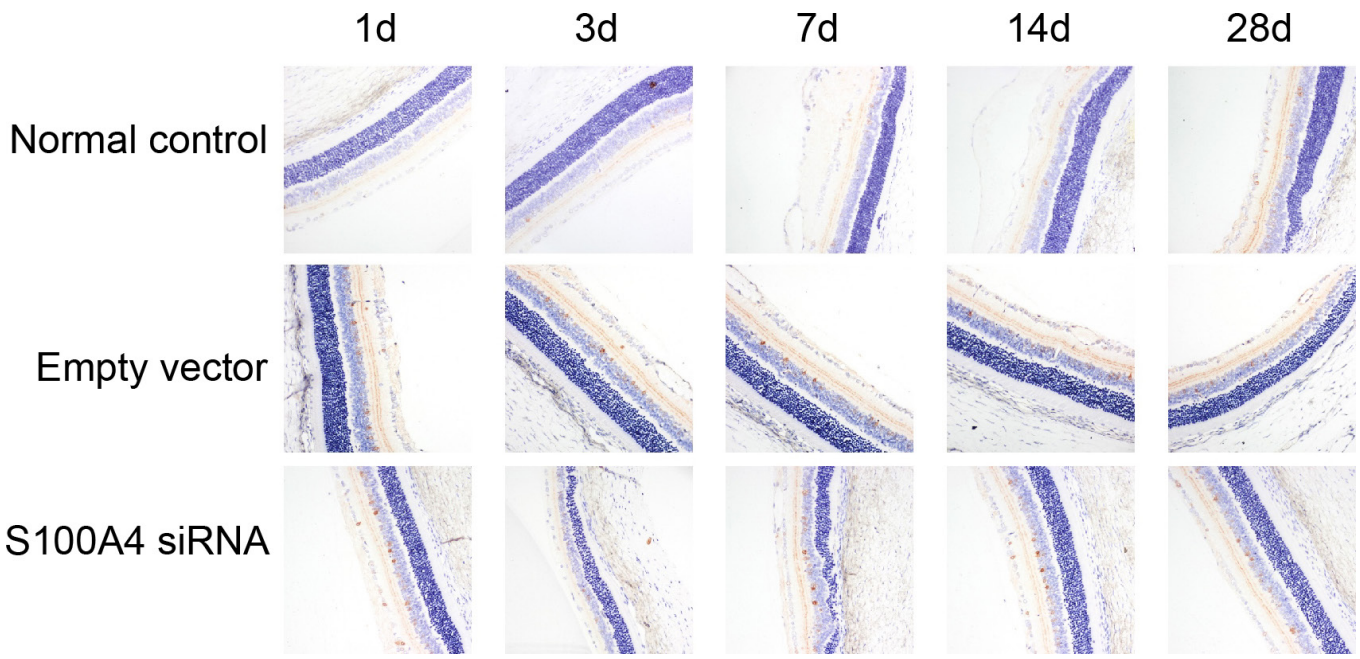

Figure 4. The protein expression of VEGF in the corneal tissues of each group by immunohistochemical detection (× 200) Notes: VEGF, vascular endothelial growth factor; the arrow indicates the brown particles as a positive signal.

gene silencing can inhibit the formation of CNV in rabbit corneal alkali burns and reduce the inflammatory reaction. S100 proteins are $Ca2^{+}$ binding low molecular mass proteins that are common in cells' homo- or heterodimers. S100 proteins display their effect by interacting with and modulating the activity of other proteins [10]. *S100A4* has been independently cloned by several research groups and was used as a marker to connect cell growth with cell movement [24]. S100A4 protein is localized in the nucleus, cytoplasm, and extracellular space of cells and has many biologic functions, such as regulating angiogenesis, cell survival, movement, and invasion [10]. Previous studies have confirmed the association between the number of *S100A4* cells and a variety of cancers, including colorectal cancer, non-small cell lung cancer, breast cancer, gastric cancer, bladder cancer, melanoma, and ovarian cancer [24]. S100A4, S100A6, S100A8, and S100A9 all have a potential role in the wound healing process; S100A4 in particular has been previously associated with corneal fibroblast regeneration [25]. A prior study proved that *S100A4* mRNA expression decreases with confluence in deficient biliary epithelial cells. This result is consistent with our study results [26]. In addition, the presence of *S100A4* in superficial and suprabasal layers demonstrated that through the normal and pterygium epithelia, it is a disease of unknown etiology with epithelial from the conjunctiva onto the cornea [25]. S100A4 and A13 are both thought to be pro-angiogenic in tumor development and have been reported to participate directly in the angiogenic process. This result is consistent with our study [7]. The study also indicated that *S100A4* may effectively reduce resistance to anti-angiogenic therapy [27]. *S100A4* is involved in the regulation of a variety of biologic effects, including cell viability, survival, and differentiation. S100A4 protein expression is also significantly decreased in inflammatory tissues and can be used as a marker of early changes in stem cell niches due to inflammation [28].

Table 3. IOD analysis of VEGF protein at different time points after alkaline burn detected by immunohistochemical staining.

Group	At 1 day	At 3 days	At 7 days	At 14 days	At 28 days
Norma control group	12.5±1.8	14.2±2.1	15.1±2.6	11.1±0.9	13.9±0.8
Empty vector group	82.1±7.3**	102.4±5.2**	151.7±13.7**	112.4±6.2**	87.1±4.2**
S100A4 siRNA group	72.5±5.5**#	88.3±9.1**##	129.5±11.0**##	97.2±8.7**##	79.7±5.3**#

Note: IOD, integral optical density. * and ** refer to $p<0.05$ and $p<0.01$ when compared with the normal control group, respectively; # and ## refer to $p<0.05$ and $p<0.01$ when compared with the empty vector group, respectively.

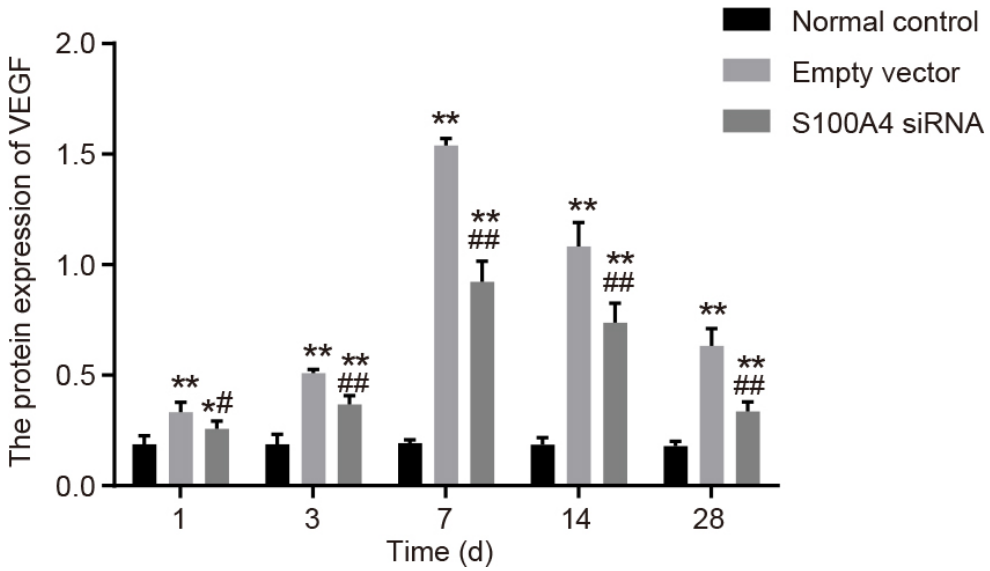

Figure 5. VEGF protein expression after alkali burn in the aqueous humor at different time points. Note: μg /l refers to protein concentration; * and ** refer to p<0.05 and p<0.01 when compared with the normal control group, respectively; # and ## refer to p<0.05 and p<0.01 when compared with the empty vector group, respectively. VEGF, vascular endothelial growth factor.

The study also found that at each time point, *S100A4* gene silencing could suppress VEGF, TNF-α mRNA, and protein expression. Furthermore, the *S100A4* gene could affect the formation of CNV in both corneal tissues and the aqueous humor by regulating the expression of VEGF and TNF-α. VEGF is a classical pro-angiogenic factor and one of the most potent endothelial cell mitogens, and it plays an important role in both angiogenesis and lymphogenesis [12]. The benefit of VEGF for vascular endothelial cells has been extensively tested in CNV-related diseases, and VEGF is characterized as having the greatest benefit in various pro-angiogenic pathways [7]. A previous study reported the correlation between the expression of VEGF and S100A4 [29]. *S100A4* gene silencing inhibits proliferation, angiogenesis, and invasion by thyroid cancer cells by downregulating the invasion of VEGF. This is in line with our study results [12]. Furthermore, *S100A4* can prolong the survival of anti-VEGF treated animals and can partially reduce glioblastoma resistance to anti-VEGF therapy [27]. TNF-α is a key cytokine involved in inflammation, immunity, cellular homeostasis, and tumor progression that exerts its effects by increasing endothelial and other inflammatory cell proliferation and activation [30]. In a previous study, it was demonstrated that TNF-α is essential in the progression of certain diseases by inducing *S100A4*.

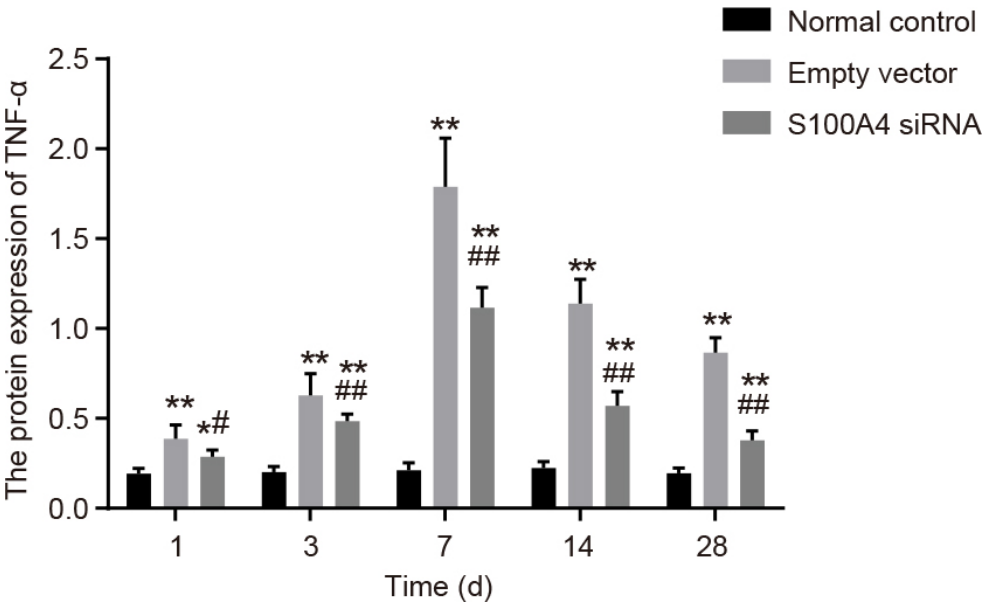

Figure 6. TNF-α protein expression at different time points in the aqueous humor after alkali burn. Notes: μg /l refers to protein concentration; * and ** refer to p<0.05 and p<0.01 when compared with the normal control group, respectively; # and ## refer to p<0.05 and p<0.01 when compared with the empty vector group, respectively. TNF, tumor necrosis factor.

This proves the results of our study [31]. *S100A4* stimulation of peripheral blood mononuclear cells (PBMCs) can significantly induce the synthesis of TNF-α. *S100A4* regulates the apoptosis and expression of TNF-α in monocytes [32]. In a previous study about cholangiocarcinoma progression, it was demonstrated that TNF-α is essential in the progression of certain diseases by inducing *S100A4*. This is in accordance with the results of our study [31].

Our study points out that *S100A4* is effective in inhibiting the formation of CNV tissues after alkali burning. This mechanism may be related to inhibiting the VEGF signaling pathway and reducing inflammation. Therefore, more research is required to provide reference for the clinical treatment of corneal alkali burns.

ACKNOWLEDGMENTS

This work was supported in part by the Health Department Science and Technology Foundation of Jiangxi Province (No: 20073027), Education Department Scientific Research Foundation of Jiangxi Province (No: GJJ10326), Jiangxi Province Natural Science Foundation (No: 2009GZY0195). The authors want to thank for all the people for their help in the paper editing.

REFERENCES

1. Zhu YF, Zheng LB, Yao YF. Impression cytological study for ocular surface disorders of late stage eye burns. Eur Rev Med Pharmacol Sci 2016; 20:605-12. [PMID: 26957260].
2. Martin LF, Rocha EM, Garcia SB, Paula JS. Topical Brazilian propolis improves corneal wound healing and inflammation in rats following alkali burns. BMC Complement Altern Med 2013; 13:337-[PMID: 24279635].
3. Colombo-Barboza M, Colombo-Barboza G, Felberg S, Dantas PE, Sato EH. Induction of corneal collagen cross-linking in experimental corneal alkali burns in rabbits. Arq Bras Oftalmol 2014; 77:310-4. [PMID: 25494378].
4. Spoler F, Forst M, Kurz H, Frentz M, Schrage NF. Dynamic analysis of chemical eye burns using high-resolution optical coherence tomography. J Biomed Opt 2007; 12:041203-[PMID: 17867792].
5. Ke Y, Wu Y, Cui X, Liu X, Yu M, Yang C, Li X. Polysaccharide hydrogel combined with mesenchymal stem cells promotes the healing of corneal alkali burn in rats. PLoS One 2015; 10:e0119725-[PMID: 25789487].
6. He J, Bazan NG, Bazan HE. Alkali-induced corneal stromal melting prevention by a novel platelet-activating factor receptor antagonist. Arch Ophthalmol 2006; 124:70-8. [PMID: 16401787].
7. Li C, Zhang F, Wang Y. S100A proteins in the pathogenesis of experimental corneal neovascularization. Mol Vis 2010; 16:2225-35. [PMID: 21139687].
8. Kubota M, Shimmura S, Kubota S, Miyashita H, Kato N, Noda K, Ozawa Y, Usui T, Ishida S, Umezawa K, Kurihara T, Tsubota K. Hydrogen and N-acetyl-L-cysteine rescue oxidative stress-induced angiogenesis in a mouse corneal alkali-burn model. Invest Ophthalmol Vis Sci 2011; 52:427-33. [PMID: 20847117].
9. Grum-Schwensen B, Klingelhofer J, Berg CH, El-Naaman C, Grigorian M, Lukanidin E, Ambartsumian N. Suppression of tumor development and metastasis formation in mice lacking the S100A4(mts1) gene. Cancer Res 2005; 65:3772-80. [PMID: 15867373].
10. Boye K, Maelandsmo GM. S100A4 and metastasis: a small actor playing many roles. Am J Pathol 2010; 176:528-35. [PMID: 20019188].
11. Oslejskova L, Grigorian M, Gay S, Neidhart M, Senolt L. The metastasis associated protein S100A4: a potential novel link to inflammation and consequent aggressive behaviour of rheumatoid arthritis synovial fibroblasts. Ann Rheum Dis 2008; 67:1499-504. [PMID: 18056757].
12. Jia W, Gao XJ, Zhang ZD, Yang ZX, Zhang G. S100A4 silencing suppresses proliferation, angiogenesis and invasion of thyroid cancer cells through downregulation of MMP-9 and VEGF. Eur Rev Med Pharmacol Sci 2013; 17:1495-508. [PMID: 23771538].
13. Zhang G, Li M, Jin J, Bai Y, Yang C. Knockdown of S100A4 decreases tumorigenesis and metastasis in osteosarcoma cells by repression of matrix metalloproteinase-9. Asian Pac J Cancer Prev 2011; 12:2075-80. [PMID: 22292654].
14. Marenholz I, Lovering RC, Heizmann CW. An update of the S100 nomenclature. Biochim Biophys Acta 2006; xxx:1282-3. [PMID: 16938360].
15. Hansen MT, Forst B, Cremers N, Quagliata L, Ambartsumian N, Grum-Schwensen B, Klingelhofer J, Abdul-Al A, Herrmann P, Osterland M, Stein U, Nielsen GH, Scherer PE, Lukanidin E, Sleeman JP, Grigorian M. A link between inflammation and metastasis: serum amyloid A1 and A3 induce metastasis, and are targets of metastasis-inducing S100A4. Oncogene 2015; 34:424-35. [PMID: 24469032].
16. Wang L, Wang X, Liang Y, Diao X, Chen Q. S100A4 promotes invasion and angiogenesis in breast cancer MDA-MB-231 cells by upregulating matrix metalloproteinase-13. Acta Biochim Pol 2012; 59:593-8. [PMID: 23162804].
17. Ochiya T, Takenaga K, Endo H. Silencing of S100A4, a metastasis-associated protein, in endothelial cells inhibits tumor angiogenesis and growth. Angiogenesis 2014; 17:17-26. [PMID: 23929008].
18. Li Y, Liu ZL, Zhang KL, Chen XY, Kong QY, Wu ML, Sun Y, Liu J, Li H. Methylation-associated silencing of S100A4 expression in human epidermal cancers. Exp Dermatol 2009; 18:842-8. [PMID: 19703228].

19. Hoffart L, Matonti F, Conrath J, Daniel L, Ridings B, Masson GS, Chavane F. Inhibition of corneal neovascularization after alkali burn: comparison of different doses of bevacizumab in monotherapy or associated with dexamethasone. Clin Experiment Ophthalmol 2010; 38:346-52. [PMID: 21077280].

20. D'Amato RJ, Loughnan MS, Flynn E, Folkman J. Thalidomide is an inhibitor of angiogenesis. Proc Natl Acad Sci USA 1994; 91:4082-5. [PMID: 7513432].

21. Lee C, Kim J, Shin SG, Hwang S. Absolute and relative QPCR quantification of plasmid copy number in Escherichia coli. J Biotechnol 2006; 123:273-80. [PMID: 16388869].

22. Pfaffl MW. A new mathematical model for relative quantification in real-time RT-PCR. Nucleic Acids Res 2001; 29:e45-[PMID: 11328886].

23. Wang Q, Yang J, Tang K, Luo L, Wang L, Tian L, Jiang Y, Feng J, Li Y, Shen B, Lv M, Huang Y. Pharmacological characteristics and efficacy of a novel anti-angiogenic antibody FD006 in corneal neovascularization. BMC Biotechnol 2014; 14:17-[PMID: 24575750].

24. O'Connell JT, Sugimoto H, Cooke VG, MacDonald BA, Mehta AI, LeBleu VS, Dewar R, Rocha RM, Brentani RR, Resnick MB, Neilson EG, Zeisberg M, Kalluri R. VEGF-A and Tenascin-C produced by S100A4+ stromal cells are important for metastatic colonization. Proc Natl Acad Sci USA 2011; 108:16002-7. [PMID: 21911392].

25. Riau AK, Wong TT, Beuerman RW, Tong L. Calcium-binding S100 protein expression in pterygium. Mol Vis 2009; 15:335-42. [PMID: 19223989].

26. Demetris AJ, Specht S, Nozaki I, Lunz JG 3rd, Stolz DB, Murase N, Wu T. Small proline-rich proteins (SPRR) function as SH3 domain ligands, increase resistance to injury and are associated with epithelial-mesenchymal transition (EMT) in cholangiocytes. J Hepatol 2008; 48:276-88. [PMID: 18155796].

27. Liang J, Piao Y, Holmes L, Fuller GN, Henry V, Tiao N, de Groot JF. Neutrophils promote the malignant glioma phenotype through S100A4. Clin Cancer Res 2014; 20:187-98. [PMID: 24240114].

28. Nubile M, Lanzini M, Calienno R, Mastropasqua R, Curcio C, Mastropasqua A, Agnifili L, Mastropasqua L. S100 A and B expression in normal and inflamed human limbus. Mol Vis 2013; 19:146-52. [PMID: 23378728].

29. Feng LZ, Zheng XY, Zhou LX, Fu B, Yu YW, Lu SC, Cao NS. Correlation between expression of S100A4 and VEGF-C, and lymph node metastasis and prognosis in gastric carcinoma. J Int Med Res 2011; 39:1333-43. [PMID: 21986134].

30. Hou CH, Yang RS, Hou SM, Tang CH. TNF-alpha increases alphavbeta3 integrin expression and migration in human chondrosarcoma cells. J Cell Physiol 2011; 226:792-9. [PMID: 20857483].

31. Techasen A, Namwat N, Loilome W, Duangkumpha K, Puapairoj A, Saya H, Yongvanit P. Tumor necrosis factor-alpha modulates epithelial mesenchymal transition mediators ZEB2 and S100A4 to promote cholangiocarcinoma progression. J Hepatobiliary Pancreat Sci 2014; 21:703-11. [PMID: 24867797].

32. Cerezo LA, Kuncova K, Mann H, Tomcik M, Zamecnik J, Lukanidin E, Neidhart M, Gay S, Grigorian M, Vencovsky J, Senolt L. The metastasis promoting protein S100A4 is increased in idiopathic inflammatory myopathies. Rheumatology (Oxford) 2011; 50:1766-72. [PMID: 21712367].

Articles are provided courtesy of Emory University and the Zhongshan Ophthalmic Center, Sun Yat-sen University, P.R. China. The print version of this article was created on 26 April 2017. This reflects all typographical corrections and errata to the article through that date. Details of any changes may be found in the online version of the article.